Generation of tunable far-infrared radiation by the interaction of a superluminous ionizing front with an electrically biased photoconductor

D. Hashimshony, A. Zigler, and K. Papadopoulos

Citation: Applied Physics Letters **74**, 1669 (1999); doi: 10.1063/1.123649
View online: http://dx.doi.org/10.1063/1.123649
View Table of Contents: http://scitation.aip.org/content/aip/journal/apl/74/12?ver=pdfcov
Published by the AIP Publishing

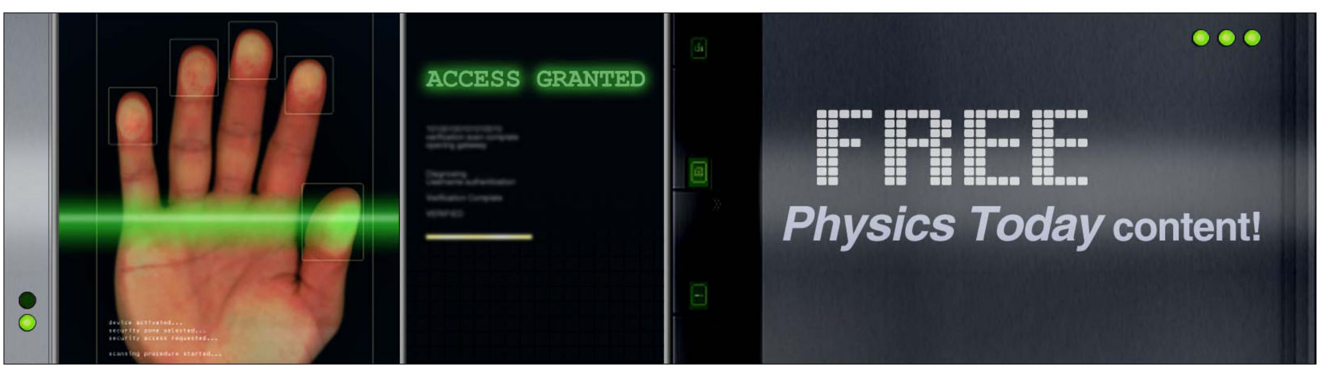

Generation of tunable far-infrared radiation by the interaction of a superluminous ionizing front with an electrically biased photoconductor

D. Hashimshony and A. Zigler[a)]
The Racah Institute of Physics, Hebrew University, Jerusalem, Israel

K. Papadopoulos
University of Maryland, College Park, Maryland 20742 and Advanced Power Technology, Inc., Washington, DC

(Received 11 November 1998; accepted for publication 25 January 1999)

Tunable radiation in the 0.1 THz to a few THz range by the interaction of a superluminous photoconducting front with an electrostatic ''frozen-wave'' configuration in a semiconductor is reported. The interaction converts the energy contained in the ''frozen wave'' into far-infrared radiation, whose frequency depends on the energy in the laser pulse creating the superluminous front and the wavelength of the static wave. © *1999 American Institute of Physics.* [S0003-6951(99)01812-4]

The THz far-infrared radiation (FIR) region of the electromagnetic spectrum has unique utility in characterizing electronic, vibrational, and compositional properties of solids, liquids, gases, flames, and flows.[1,2] The availability of femtosecond lasers has recently led to the development of new types of THz sources based on the principle of dc to ac conversion. Powerful, broadband THz radiation was generated by the incidence of 100 fs laser pulses on large aperture monotonically biased photoconductors, such as GaAs.[1–5] The broadband radiation pattern generated by this technique has very little gain and its center frequency is controlled only by the laser pulse length and the relaxation properties of the carriers. Two physical mechanisms have been advanced as the source of the radiation: photoconduction[4,5] and optical rectification.[3,4] In the former case, the physics underlying the process involves transfer of the stored electrostatic energy to radiation through interaction of the laser with the surface of the photoconductors. In the latter case, part of the laser energy is converted to radiation through the interaction with the electro-optic crystal.

Generation of short bursts of radiation in the lower-frequency range between 5 and 20 GHz was recently reported.[6] The interaction of the subluminous front with the frozen wave resulted in the emission of an upshifted radiation. The process closely parallels the well-studied process of the Doppler frequency upshift by the interaction of a moving relativistic ionization front with an impinging electromagnetic wave.[7,8]

In this letter we present a proof-of-principle experiment of a radiation process whose underlying physics combines elements of the approaches described previously. This is accomplished by using the volume rather than the surface interaction between the laser and the charged photoconducting configuration and generation of the transient radiation inside a plasma rather than in free space. These require that the emitted radiation frequency is consistent with the dispersion properties of the plasma generated in the photoconductor volume and the generated wavelength consistent with a number of the frozen waves involved in the interaction. Primary control of the radiation frequency is adjusting the plasma frequency, which is a linear function of the energy in the laser pulse. The radiation bandwidth is a function of the number of frozen waves contained in the photoconductor.

The experimental configuration is shown in Fig. 1. It has three components. The electrically biased ZnSe photoconductor radiating structure, a Ti–sapphire 100 fs laser, and a radiation detector. The carrier generation involves two photons and the absorption depth is intensity dependent. This allows for deeper penetration of the laser radiation and creation of a large volume of carriers resulting in a volume interaction of the front with the bias rather than the surface interaction occurring in the large aperture antennas we referred to previously.

The crystal was placed between the two thin glass plates with a multiple electrode structure made by deposition of an Al structure on the plates. The capacitor plates were 3 mm by 10 mm, separated by a distance of 3 mm. Thus, the initial static-wave wavelength was centered at 9 mm. The capacitor plates were extended over the crystal to create a uniform

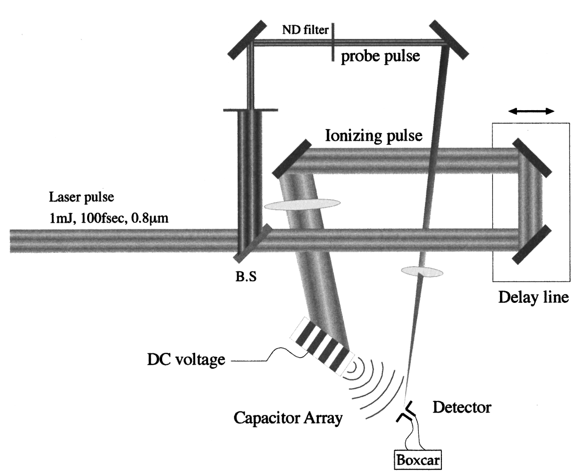

FIG. 1. Schematic diagram of the experimental setup.

[a)]Electronic mail: zigler@vms.huji.ac.il

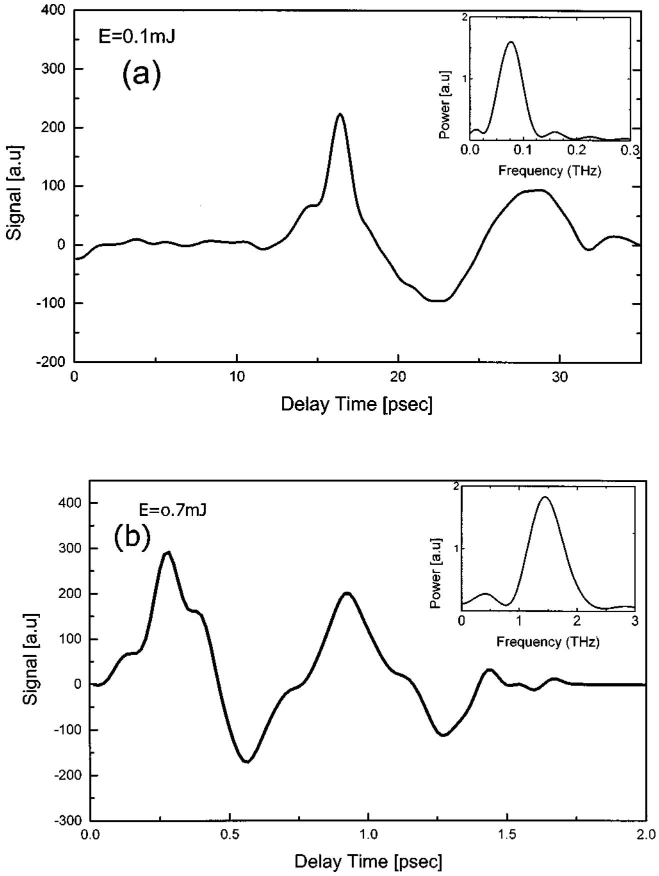

FIG. 2. Measured signals for laser energy of (a) 0.1 mJ and (b) 0.7 mJ. The insets show the power spectrum of the corresponding signals.

field inside the crystal. The capacitors were alternately biased with a voltage of 50 V to form a frozen-wave configuration.

The THz radiation was generated by sweeping a 100 fs laser pulse at an oblique angle of incidence on the crystal. A Ti:sapphire laser operating at 0.8 μ wavelength, whose energy was limited to 2 mJ, and with a repetition rate 10 Hz was used. The wave form of the radiated electric field was measured using the standard pump and probe technique.[9] A gated planar dipole antenna monitored the amplitude of the radiated electric field. The antenna was constructed on a heavily ion-implanted silicon layer on a sapphire substrate, resulting in a subpicosecond temporal response.[10] This antenna was driven by the radiation from the capacitor array and gated at different delay times by varying the optical delay between the pump and probe laser pulses. The amplitude of the induced, time-dependent voltage across the gap was determined by measuring the average current produced in the antenna circuit using a gated boxcar integrator. The maximum frequency response of the configuration was approximately 2 THz, dictated by the carrier lifetime of < 0.5 ps. The profile of the radiation electric field was determined by monitoring the average current versus the time delay between the pump laser beam and the probe laser beam.

Two measured temporal scans of the emitted radiation electric field at different laser energies are shown in Figs. 2(a) and 2(b). The scan represents the measured signal intensity versus the delay between the pump and the probe laser pulse. The insets show the power spectrum of the corresponding signals.

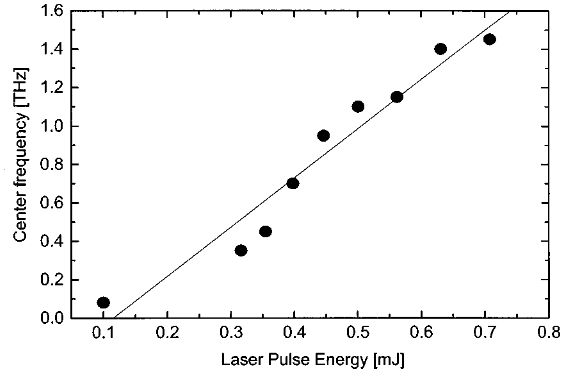

FIG. 3. Center frequency of emitted radiation vs laser pulse energy.

By a careful examination of Figs. 2(a) and 2(b), the collective nature of the interaction and the analogy with the frozen-wave generator becomes apparent. It can be seen that the first half-cycle peak of the emitted wave form is much narrower and sharper then the following peak. A possible explanation of this effect can be that, in the time-domain scan each half cycle can be considered as the footprint of one of the capacitors, where the first one to be measured in free space is the last one to be generated. The radiation created by the last capacitor is less affected by the plasma and by destructive interference, since it is radiated almost directly in free space. The following half cycles of radiation were originally generated deeper inside the plasma and effected more by the plasma presence and the interference between sources. Their contribution to the radiation measured outside cannot be considered as purely generated by one capacitor alone but is a result of the interference among the sources.

A plot of the measured frequency as a function of the laser pulse energy in the range between 0.1 and 1 mJ is shown in Fig. 3. The experimental points were derived following the procedure outlined above. It is clear that the frequency of the radiation scales linearly with the energy in the laser pulse. As will be discussed later, the carrier density generated, or equivalently, the plasma frequency, is proportional to the pulse energy.

In interpreting and scaling the above results it is instructive to refer to the traditional frozen-wave generator concept.[11] Such a device consists of segments of transmission line sections with one-way transit times equal to the desired microwave half period arranged in series or parallel and connected with optically activated switches. The sections are charged alternatively positive and negative to form a dc ''frozen wave.'' Radiation is produced when the optically controlled switches are activated simultaneously. The critical differences in the physics controlling our device and the traditional frozen-wave generator, is that the shorting of the capacitor array is sequential, however, the resultant radiation propagates inside the plasma which is generated at superluminous speeds. This has profound consequences since the frequency is upshifted to satisfy the appropriate dispersion relation and phase-matching conditions. Following Lampe, Ott, and Walker it can be shown the generated wave must satisfy

$$(k_0 c\beta-\omega)^2-\omega^2\epsilon\beta^2+\omega_e^2\epsilon\beta^2\frac{\omega}{\omega-i\gamma}=0, \tag{1}$$

where $\beta=1/\sin\theta$, $k_0=\pi/d$ where d is the distance between the capacitors, θ is the incidence angle of the laser, ϵ is the dielectric constant of the semiconductor, ω_e the plasma frequency, and γ the phenomenological dephasing rate.[4] It is easy to see that in the absence of plasma, i.e., $\omega_e\Rightarrow 0$ (or $\omega \gg \omega_e$), Eq. (1) reduces to the frozen generator one. However, for $k_0 c\beta \ll \omega$ Eq. (1) becomes $\omega(\omega - i\gamma)=\omega_e^2\epsilon\beta^2/(\epsilon\beta^2-1)$. It is clear that for $\omega_e \gg \gamma$ and $\epsilon\beta^2 \gg 1$, conditions easily fulfilled in our experiment, the emitted frequency ω is near the plasma frequency and proportional to $\sqrt{n}$, where n is the carrier density. The value of n is, of course, a function of the laser energy per pulse E. It is easy to see that for two-photon absorption, since the absorption length is $(\alpha I)^{-1}$, where I is the laser intensity and α the two-photon absorption coefficient, the average density is given by $n=\alpha E^2/h\nu S^2\tau$, where h is the Planck constant, ν is the laser frequency, S is the illuminated area of the crystal, and τ the laser pulse length. Therefore, we find that the emitted frequency scales linearly with the laser pulse energy, consistent with the results shown in Fig. 3.

Before closing, we comment on the scaling properties of the concept presented with respect to power, frequency, and bandwidth. As noted in Lampe, Ott, and Walker for superluminous fronts, the transmission coefficient is close to unity. As a result, the output radiation has a field amplitude close to the static field. During the sweep time, the electrostatic energy stored in the photoconductor is transformed into electromagnetic radiation, providing a potential for producing high-power radiation. Frequency tunability scaling is a linear function of E, indicating the possibility to scale frequencies up to 10 THz with relatively modest laser energies. Finally, the bandwidth is controlled by the number of capacitors N so that $\Delta\omega/\omega=1/N$. Besides using longer lengths, the bandwidth can be significantly decreased by implementing phased array concepts.

We have presented a proof-of-principle experiment of a radiation concept that can generate tunable, ''narrowband'' generation spanning the range of 100 GHz to the FIR. The use of photoconductors provides several advantages: the high breakdown threshold allows significant energy storage that may be converted to a substantial radiated power. The small energy band gap reduces the required ionization energy. Finally, the short recombination time allows a high repetition rate. The concept is fully scalable and has the potential for providing powerful, tunable sources in a frequency range valuable for many spectroscopic applications.

[1] D. Grischkowsky, S. Keiding, M. van Exter, and Ch. Fattinger, J. Opt. Soc. Am. B **7**, 2006 (1990).
[2] B. I. Greene, P. N. Saeta, D. R. Dykaar, S. Schmitt-Rink, and S. L. Chuang, IEEE J. Quantum Electron. **JQE-28**, 2302 (1992).
[3] D. H. Auston, K. P. Cheung, J. A. Valdmanis, and D. A. Kleinman, Phys. Rev. Lett. **53**, 1555 (1984).
[4] X. C. Zhang and Y. Jin, Perspect. Optoelectron. **3**, 81 (1995).
[5] X. C. Zhang, B. B. Hu, J. T. Darrow, and D. J. Auston, Appl. Phys. Lett. **56**, 1011 (1990).
[6] W. B. Mori, T. Katsouleas, J. M. Dawson, and C. H. Lai, Phys. Rev. Lett. **74**, 542 (1995).
[7] V. I. Semenova, Sov. Radiophys. **10**, 599 (1967).
[8] M. Lampe, E. Ott, and J. H. Walker, Phys. Fluids **10**, 42 (1978).
[9] M. van Exter, Ch. Fattinger, and D. Grischkowsky, Appl. Phys. Lett. **55**, 24 (1989).
[10] F. E. Doany, D. Grischkowsky, and C.-C. Chi, Appl. Phys. Lett. **50**, (1987).
[11] W. Nunnaly, IEEE Trans. Electron Devices **37**, 2439 (1990).